Meng et al. The Journal of Global Positioning Systems (2018) 16:4
https://doi.org/10.1186/s41445-018-0014-7

The Journal of Global Positioning Systems

ORIGINAL ARTICLE Open Access

Dynamic characteristic of the forth road bridge estimated with GeoSHM

Xiaolin Meng[1*], Ruijie Xi[1,2] and Yilin Xie[1]

Abstract

The importance of bridge health monitoring and management has been recognized by authorities of long-span bridges throughout the world in recent years. The GeoSHM consortium, led by the University of Nottingham, was awarded a Feasibility Study (FS) grant in 2013 by the European Space Agency (ESA) to investigate how to use integrated GNSS and Earth Observation technologies for the structural health monitoring of large bridges. During the GeoSHM FS period a small monitoring system was installed on the Forth Road Bridge in Scotland and the consortium have gathered huge data sets and rich experience regarding the design and implementation of GeoSHM according to essential user needs. This paper, based on the data from GNSS receivers installed on the two middle span sites and top of the southern tower of the Forth Road Bridge, intends to reveal the dynamic characteristics of the bridge. By using a moving average filter, Fast Fourier Transformation (FFT) and the peak-picking approach, the three-dimensional (3D) displacement time series under ambient excitation were decomposed into long-period movement and dynamic vibration response. The results demonstrate that the movement of the Forth Road Bridge in lateral direction is mainly caused by wind loading, and the correlation is about 0.7. In vertical direction, the displacements of middle span sites under the normal traffic loadings can reach 0.3 m and because of the main cable linking the middle span and top of the tower, the longitudinal movement of the southern tower top site has a high correlation with the vertical displacements of middle span sites. It has been found that due to the stiffness of the tower the trend terms inside lateral and vertical time series mainly consist of multipath effect and quasi-static displacement. The dynamic vibration frequencies and corresponding motion amplitudes were also extracted. It is found that the first natural frequencies of the middle span of the Forth Road Bridge are 0.065 Hz, 0.15 Hz and 0.104 Hz for lateral, longitudinal and vertical directions, respectively. For the south tower, vibration frequencies of 0.18 Hz can be seen in all three directions, but 0.104 Hz is only visible in longitudinal component because of the cables linking the tower and middle span. It demonstrates that with a proper data mining approach both the low frequency responses and dynamic vibration characteristics of a large bridge under ambient loadings can be extracted from GNSS data sets. Thus, GeoSHM can be used by bridge owners as an effective tool to assess the operational conditions of the bridge.

Keywords: GeoSHM, Displacement monitoring, The forth road bridge, Peak-picking approach, Dynamic characteristics, Ambient excitation

* Correspondence: xiaolin.meng@nottingham.ac.uk
[1]Nottingham Geospatial Institute, The University of Nottingham, Nottingham NG7 2TU, UK
Full list of author information is available at the end of the article

Fig. 1 The Forth Road Bridge in the UK

Introduction

Global Navigation Satellite Systems (GNSS), especially Global Positioning System (GPS) technology has been employed to monitor large bridge deformation for more than 20 years (Meng 2002). Compared with traditional techniques, GNSS can provide continuous, automated, all-weather and highly accurate measurements while it is difficult for other sensors such as an accelerometer to detect both the static and dynamic deformations of the structure (Meng et al. 2004; Meng et al. 2006; Li et al. 2006; Yi et al. 2013; Yu et al. 2016). GNSS techniques can be used effectively to monitor long suspension/cable-stayed and medium bridges (Xu et al. 2002; Watson et al. 2007; Roberts et al., 2012; Yu et al. 2014).

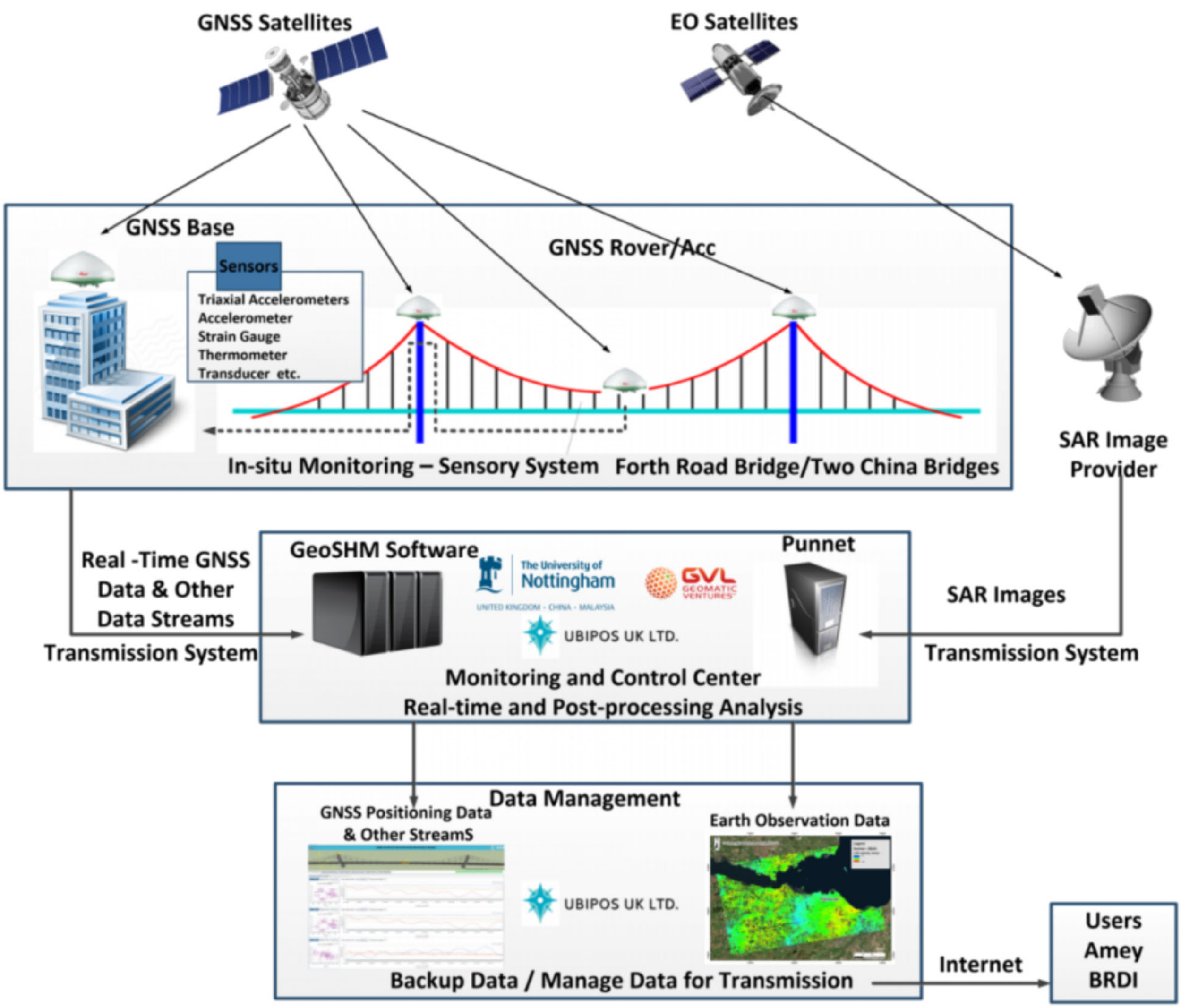

Fig. 2 The overall GeoSHM system architecture

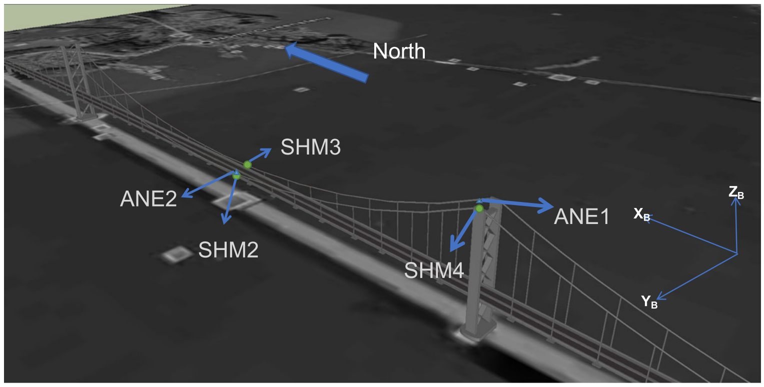

Fig. 3 The GNSS receiver distribution and the defined bridge coordinate system

Many technical issues have also been addressed, such as the impact of GPS satellite and pseudolite geometry on structure deformation monitoring (Meng et al. 2004), dynamic multipath in structural health monitoring of bridges (Moschas and Stiros, 2014), bridge monitoring with high frequency GPS (Roberts et al., 2004), and using RTK-GPS to measure wind-induced response (Tamura et al. 2002), etc.

However, there are obvious disadvantages of using GNSS to monitor bridge deformation. For example, the low sampling rate and high level of observation noise make it impossible to detect relatively high vibration bridge frequencies (Meng 2002; Meng et al. 2007; Breuer et al. 2015; Górski, 2017). Thus, many researches have made to use an integrated monitoring system with dual frequency GNSS receivers and accelerometers to detect the dynamics information which can significantly improve the overall system performance (Roberts et al., 2001; Yu et al. 2014; Meng et al. 2014). Meng et al. (2014) presented an optimal GPS/accelerometer integration algorithm for monitoring the vertical structural dynamics. Moschas and Stiros (2011) also achieved the dynamic displacements and modal frequencies of a short-span pedestrian bridge using GPS and an/the accelerometer. Xiong et al. (2017) proposed an AFEC mixed filtering algorithm to eliminate the multipath errors and random noise from GNSS and accelerometer data.

GNSS receivers and accelerometers, nevertheless, can only determine the bridge responding information. Enough data on loading and responding should also be collected if we want to correctly assess the health of bridge (Sumitoro et al., 2011; Erdoğan and Gülal, 2009; Meng et al. 2016). Thus, an integral management system with different sensors to measure (mainly GNSS, interferometric SAR, accelerometer) and quantify the induced excitation (wind, traffic and even earthquakes etc.) and its corresponding response, is important and needs to be carefully designed. The GeoSHM (GNSS and Earth Observation for Structural Health Monitoring of Bridges) project supported by the European Space Agency is a system that uses integrated GNSS and Earth Observation technologies for structural health monitoring of large bridges – and in its feasibility study the consortium used the Forth Road Bridge in Scotland as its testbed bridge. In the FS stage from August 2013 to March 2015, we installed a small footprint sensor system on the bridge (Meng et al. 2016). In the demonstration

Fig. 4 GeoSHM antenna setting-ups at monitoring stations

Table 1 The details of the monitoring stations

Station Name	Location	Baseline Length (m)	Sampling (Hz)	Receivers (antenna)
SHM2	Middle Span	1528.09	20	Leica Geosystem GR10 (LEIAR10)
SHM3	Middle Span	1527.97	20	Leica Geosystem GR10 (LEIAR10)
SHM4	South Tower	1032.67	20	Leica Geosystem GR10 (LEIAR10)

stage from March 2016 to Mach 2018, we are focusing on addressing the major drawbacks of the GeoSHM FS Project and developing a smart data strategy to fully reflect the end user needs.

In this paper, we will use the GNSS receivers installed on the middle span and top of the tower of the Forth Road Bridge in the GeoSHM project to investigate the dynamic characteristics of the bridge. Based on FFT and the peak-picking approach, the displacements time series under ambient excitation were decomposed into long-period movement and dynamic vibration response, and the mechanism of the movement and the natural frequencies were also analysed.

Forth road bridge and GeoSHM

The Forth Road Bridge crosses the Firth of Forth and links the north of Scotland with Edinburgh and the south of the A90 road. The bridge length is 2.5 km and the main span length is 1006 m. It opened in 1964 and the traffic volume has already surpassed 24 million vehicles per annum, around 11 times of the traffic volume in 1965. Fig 1 is the picture of the Forth Road Bridge.

The main aim of the GeoSHM is to use different kinds of sensors to measure (mainly GNSS, interferometric SAR, accelerometer) and quantify the induced excitation (wind, traffic and even earthquakes etc.) and its corresponding response, and make comparisons with theoretically designed thresholds or models of the structure for the evaluation of the health condition of bridges (Meng et al. 2016).

Figure 2 shows the overall structure of GeoSHM that consists of a sensor network, a data transmission module and sub-systems for data processing and visualisation. The sensor system consists of: one reference GNSS station set on the top of the office building of the Forth Road Bridge, three monitoring GNSS stations with two sets on each side of the middle span and one set on the west side of southern tower, and two ultrasonic anemometers with one on the west side of middle span and the other close to southern tower site. Figure 3 shows the distribution of the sensors and Fig. 4 gives the GNSS antennas and the anemometers located at the middle span and top of the tower. More details about monitoring

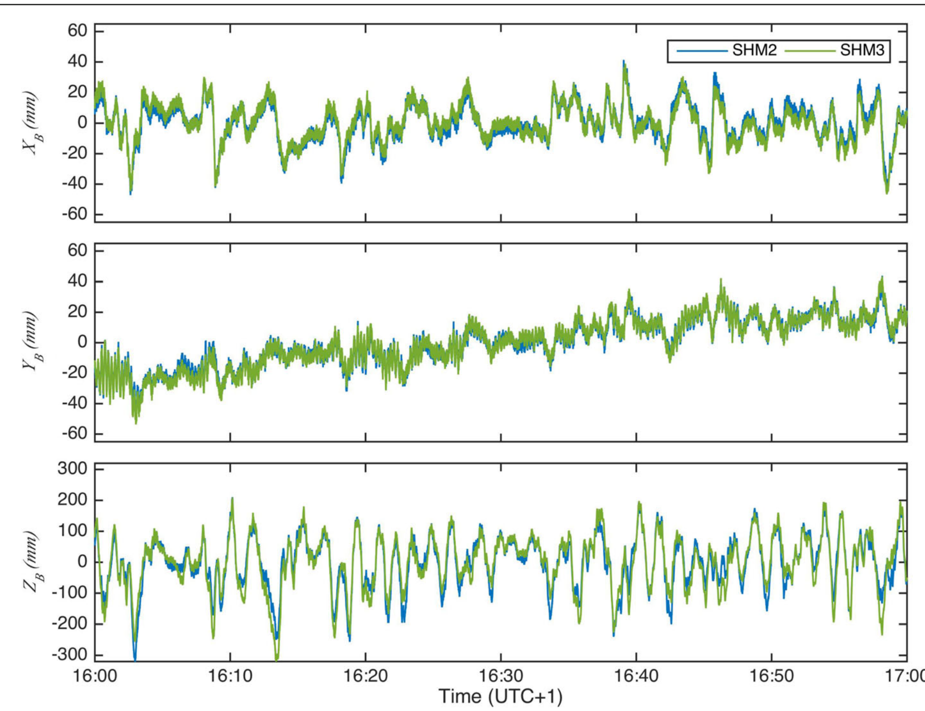

Fig. 5 Displacement time series of Middle span

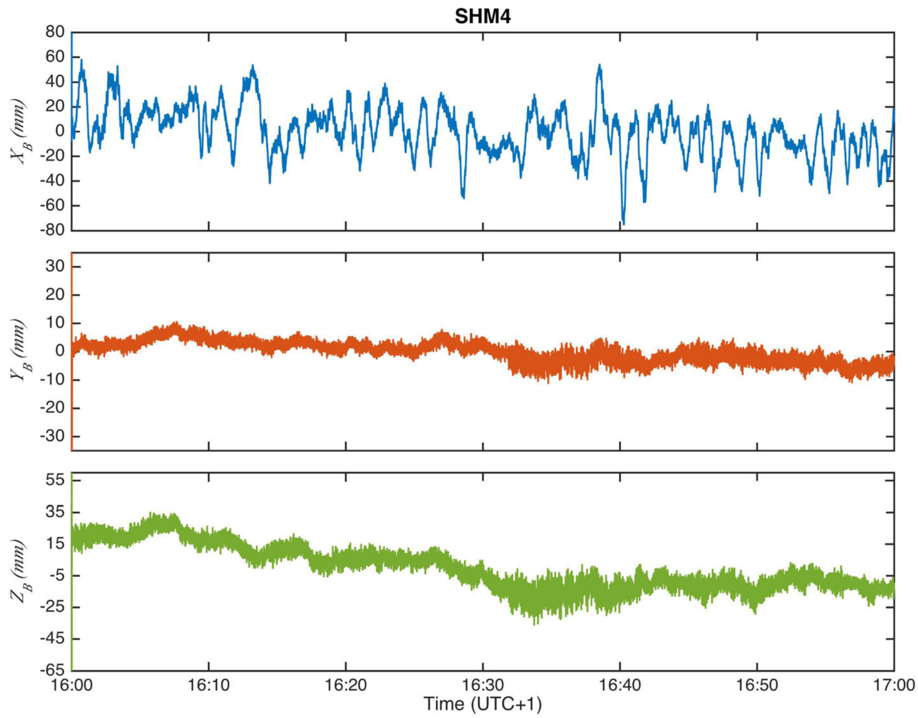

Fig. 6 Displacement time series of top of the tower

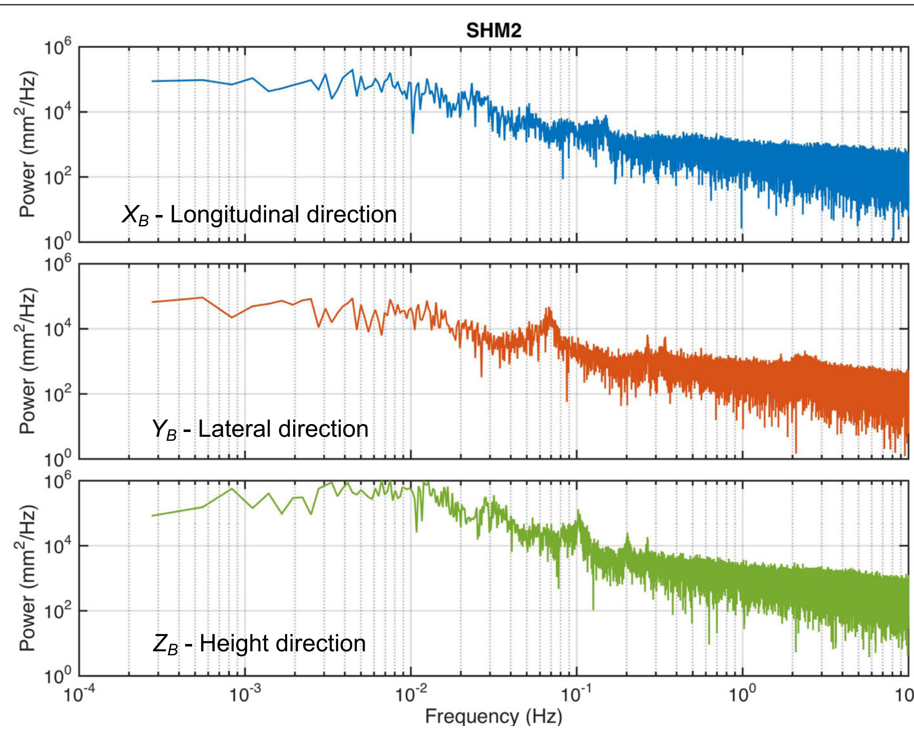

Fig. 7 FFT result of SHM2

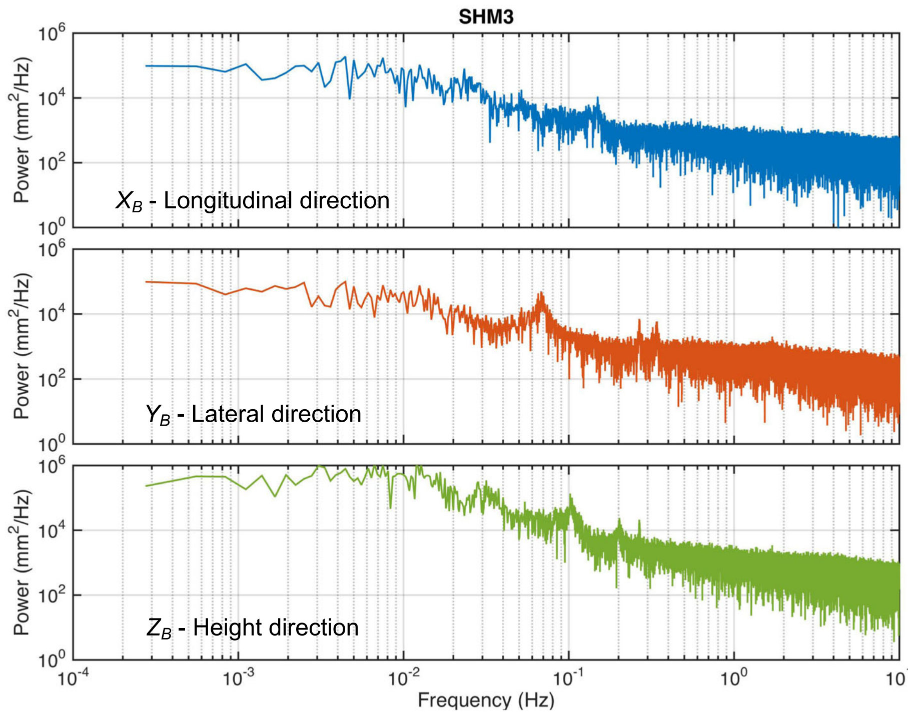

Fig. 8 FFT result of SHM3

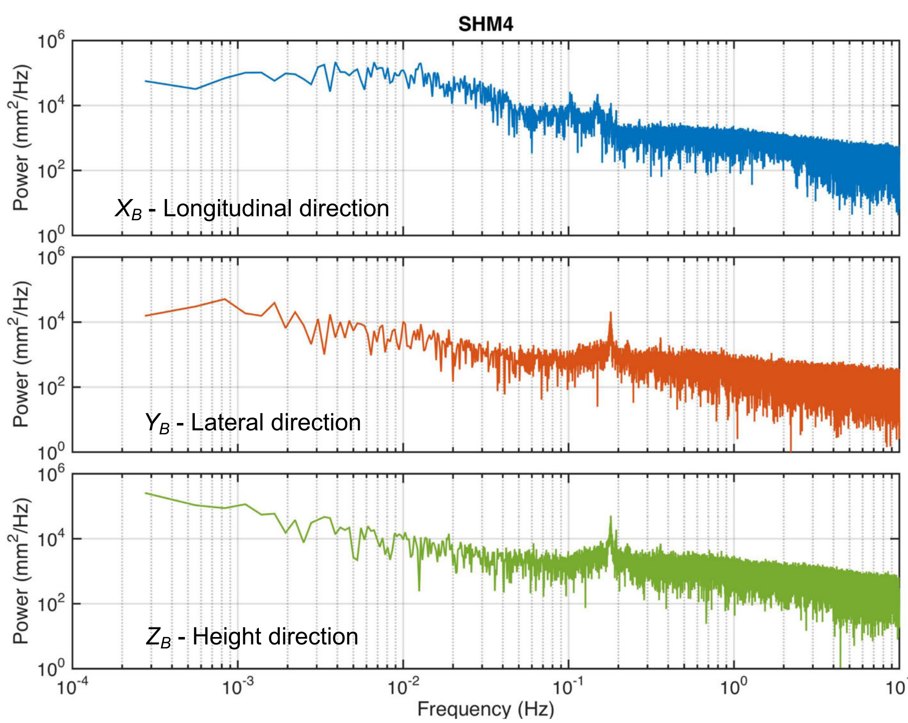

Fig. 9 FFT result of SHM4

Table 2 Dominant frequencies detected from displacement time series. (Hz)

Station Name	Lateral (Y_B)	Longitudinal (X_B)	Height (Z_B)
SHM2	0.065 0.268 0.342 1.702	0.15	0.104 0.205 0.268
SHM3	0.065 0.268 0.342 1.702	0.15	0.104 0.205 0.268
SHM4	0.18	0.104 0.15 0.18	0.18

stations can be seen in Table 1. Automated data acquisition is carried out by these sensors and the acquired real-time data are sent, via the optic fibre network laid underneath the bridge, to a local hub before they are streamed to the data processing centre set up at the University of Nottingham via public Internet. The received raw data sets are processed in real time or a post-processing manner.

Methods

GPS data processing

As previously mentioned, the GNSS data collected can be processed in real-time and post-processing manner modes. In this paper, Real-Time Kinematic (RTK) mode was applied to obtain displacement time series of monitoring stations (Elnabwy et al. 2013).

Since the short baselines are used (Table 1) in GNSS data processing, the satellite-dependent terms, such as satellite clock offsets, and carrier phase fractional biases, the distance-dependent terms, such as tropospheric and ionospheric delay, and satellite orbit errors could be neglected in double-difference (Breuer et al. 2015; Górski, 2017). Thus, there are only coordinate parameters and double-difference ambiguity parameters left in the parameter list to be estimated. For the purpose of fast ambiguity fixing, dual-frequency phase observations are used. The unknown parameters are estimated by a Kalman filter, and the coordinate parameters with float ambiguities can be obtained. Then the LAMBDA method will be applied to obtain the ambiguity fixed resolutions. During the data processing, the broadcast ephemeris was used to calculate the orbit of satellites. The elevation cutoff angle was set to 10°, and the elevation related stochastic model was used for weighting the random observation errors.

The outputs of the GNSS software were instantaneous Cartesian coordinates of monitoring stations in the WGS84 coordinate system (X, Y, Z) and the baseline components (N, E, U) formed from each monitoring station to the reference station SHM1. However, a local Bridge Coordinate System (BCS) (X_B, Y_B, Z_B) should be defined for analysis purpose (Meng et al. 2016). X_B axis was formed by SHM2 and SHM4 and points to the longitudinal direction of the bridge as shown in Fig. 3.

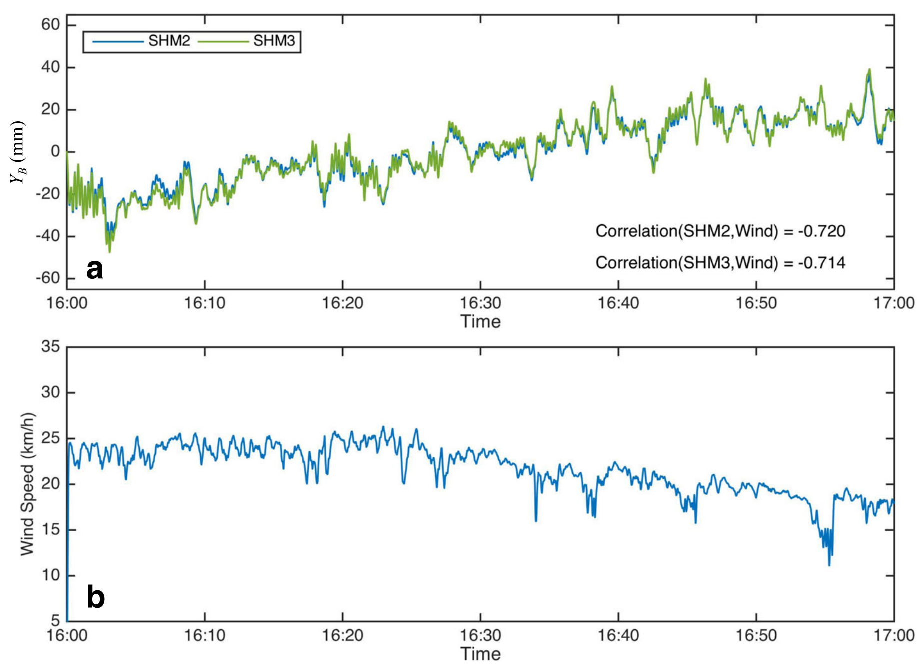

Fig. 10 a Long-period movement component for middle span and (**b**) wind speed time series in lateral (Y_B) component. The correlation coefficients between displacement and wind speed time series are shown in the figure (**a**)

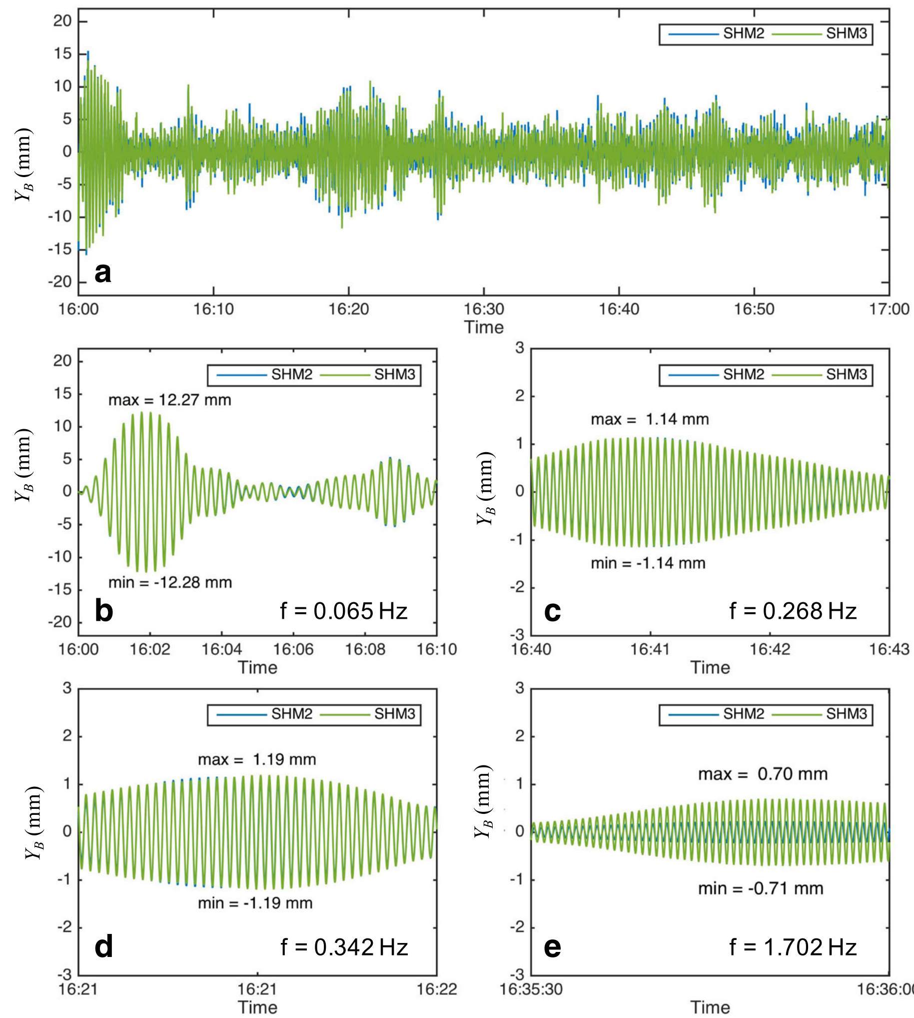

Fig. 11 Dynamic vibration response of middle span and corresponding dominant frequency signal extracted in lateral (Y_B) component

Then, Y_B and Z_B are correspond to the lateral and height directions. Coordinates in BCS can be obtained by transforming from WGS84 with 2D similarity transformation (Eq. (1)). The azimuth of the bridge is defined α.

$$\begin{pmatrix} X_B \\ Y_B \\ Z_B \end{pmatrix} = \begin{pmatrix} \cos a & \sin a & 0 \\ -\sin a & \cos a & 0 \\ 0 & 0 & 1 \end{pmatrix} \begin{pmatrix} N \\ E \\ U \end{pmatrix} \tag{1}$$

In terms of displacement time series, the mean values can be removed by Eq. (2) to limit the displacements in all components around zero.

$$\begin{pmatrix} dX_{Bi} \\ dY_{Bi} \\ dZ_{Bi} \end{pmatrix} = \begin{pmatrix} X_{Bi} \\ Y_{Bi} \\ Z_{Bi} \end{pmatrix} - \frac{1}{n} \sum \begin{pmatrix} X_{Bi} \\ Y_{Bi} \\ Z_{Bi} \end{pmatrix} \tag{2}$$

where (dX_{Bi}, dY_{Bi}, dZ_{Bi}) are the displacements over every recording interval, n represents the total number of the observation epochs, and ($i = 1, 2, \ldots, n$).

Frequency domain decomposition with peak-picking approach

In general, displacement time series in the ith direction $\delta_i(t)$ of a structure in time t can be expressed as follows (Hristopulos et al. 2007; Erdoğan and Gülal, 2009):

$$\delta_i(t) = m_i(t) + d_i(t) + n_i(t), \quad t \in \{t_1, t_2, \rightleftharpoons, t_N\} \tag{3}$$

where $m_i(t)$ is the long-period component or low frequency response of the time series, $d_i(t)$ is the dynamic vibration component, and $n_i(t)$ is random noise from various sources. Then, a filtering procedure is applied to the series so as to partially eliminate the effect of noise in the series and to analyse the mechanism of the low frequency trend and demonstrate the periodic components. In this paper, a simple moving average filter with a step of approximately 4 s (Moschas and Stiros 2011)

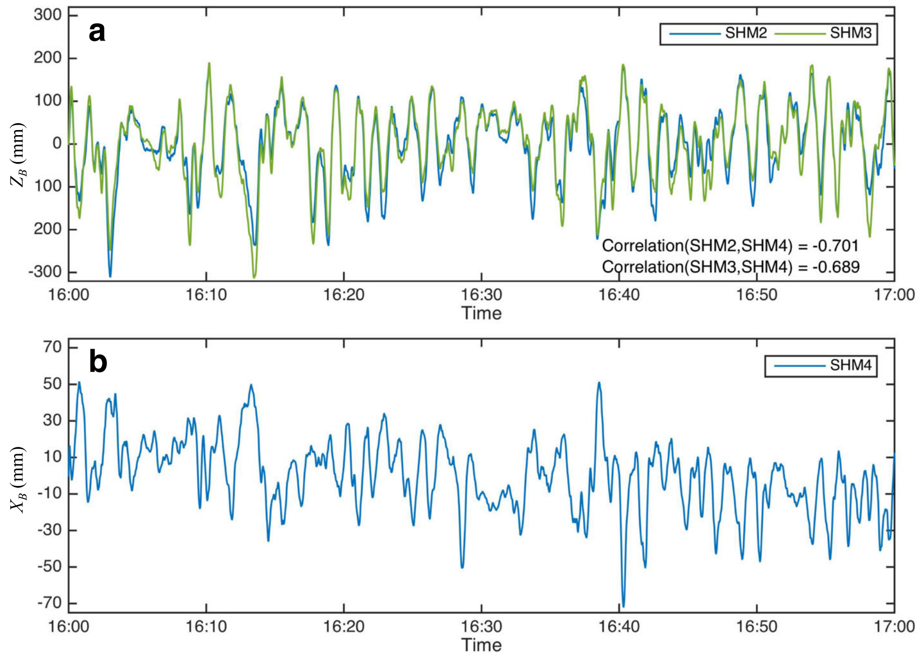

Fig. 12 Long-term movement component for middle span in height (Z_B) component and for top of the tower in longitudinal (X_B) component

was employed to separate the long-period component of the time series $m_i(t)$.

After the long-period component analysis, the dynamic vibration response $d_i(t)$ should be extracted by a proper digital filter. In this paper, a peak-picking approach for extracting structural vibration frequencies and corresponding amplitudes proposed by Meng et al. (2007) was used. This approach consists of a FFT algorithm for precisely detecting local dominant frequencies and a Chebyshev type I digital bandpass filter for identifying specific frequencies and the corresponding vibration amplitude of the frequencies (Meng et al. 2007).

Results

This section demonstrates the long-period response of the bridge and the detection frequencies from ambient vibration, and corresponding amplitude, using the above-mentioned peak-picking approach.

Monitoring results and preliminary analysis

In this paper, the data from July 25th 2017 were selected to do the displacement analysis. By taking the high sampling rate of GNSS data into consideration, the results from 16:00 to 17:00 are shown in the following.

Figures 5 and 6 plot the time series of the station displacements at the middle span and top of the tower. As it is shown, vibrations happened obviously in all three directions. The changeable ranges in the longitudinal (X_B) and height (Z_B) direction were within 5 cm and 30 cm, respectively. The displacements in the lateral (Y_B) direction were smaller in the amplitude of about 8 cm. However, a rising trend can be obviously seen. It may be a result of the wind loading.

As for SHM4, at the top of the tower, only the longitudinal (X_B) direction shows a high amplitude displacement with about 6 cm. In the lateral (Y_B) and height (Z_B) directions, the quasi-static displacements and high frequency noise can be observed. It also should be noticed that the amplitude between 16:30 and 16:40 becomes higher.

The displacements shown in Figs 5 and 6 were analysed by the FFT (Figs 7, 8 and 9). From Figs. 7, 8 and 9, the local dominant frequencies can be identified and extracted, which are listed in Table 2. From the table, we can see that SHM2 and SHM3 shared the same dominant frequencies in all directions. That is because they are just located at both sides of the middle span. SHM4 had one dominant frequency (0.18 Hz), in three directions, different from those of middle span, which is the natural frequency for the tower. The other two frequencies can also be found in the middle span, which will be explained in section 4.2.

Low frequency response and dynamic vibration analysis

In this section, the displacement time series were decomposed into low frequency response (Long-period component: including quasi-static displacement and background noise) and dynamic vibration signal (Short-period component: contains the dynamic displacement of the oscillation signal plus multipath noise). The long-period component

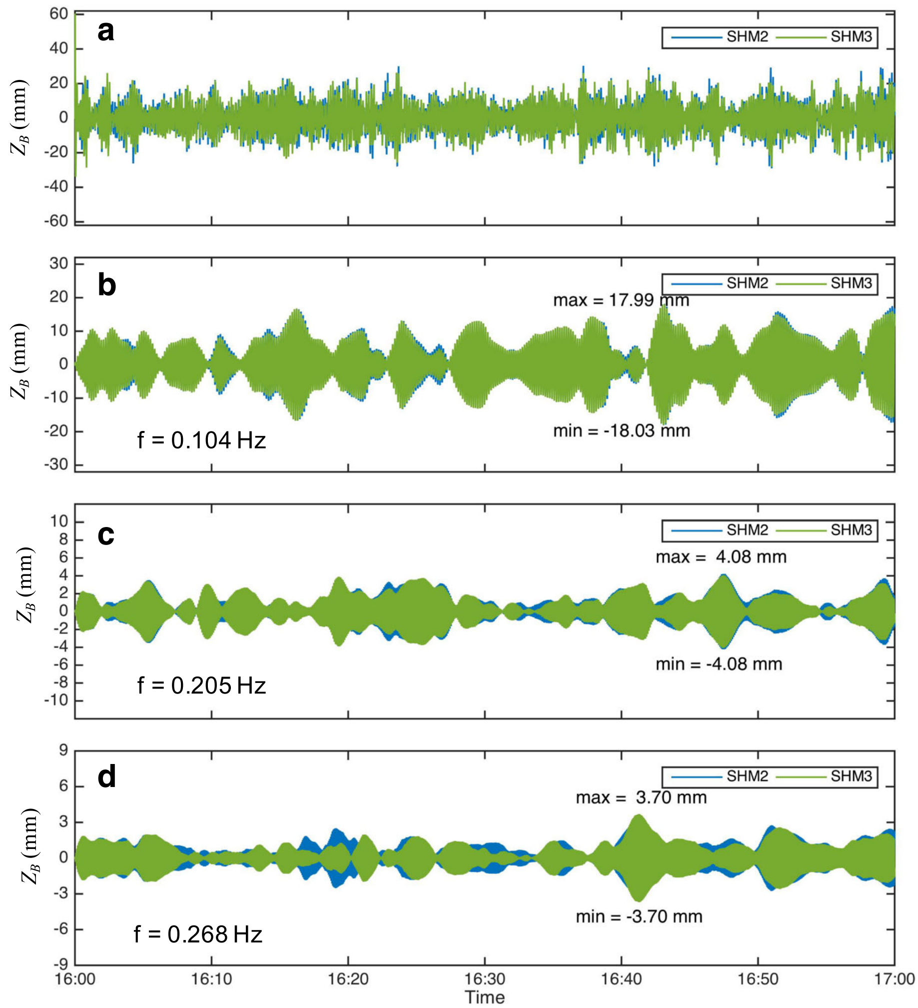

Fig. 13 Dynamic vibration response of middle span and corresponding dominant frequency signal in height (Z_B) component

was obtained by a moving average filter and the dynamic vibration responses were extracted by the eight-order Type 1 Chebyshev bandpass digital filters with pass-band and stop-band frequencies. The pass-band ripple is 1 dB.

Figure 10a shows the long-period component of the displacement at middle span in lateral (Y_B) direction. It can be seen that the time series of two monitoring sites match well with each other. That means the middle span moves as a whole body under the loads. Figure 10b gives the wind speed in the same session. To better understand the relationship between displacements and wind loadings, the correlation coefficient between them was calculated by Eq. (4)

$$R(x,y) = \frac{\sum_{i=1}^{n}(x_i-\overline{x})(y_i-\overline{y})}{\sqrt{\sum_{i=1}^{n}(x_i-\overline{x})^2\sum_{i=1}^{n}(y_i-\overline{y})^2}} \tag{4}$$

where n is the length of the time series,($i = 1,2,\ldots,n$), and $\overline{x}, \overline{y}$ are the mean value of time series x,y. We can see that the correlation coefficient between the two displacement time series and wind series are – 0.72 and – 0.714, which means the movements of the middle span have a high correlation with the wind. During this hour, the wind direction was against the Y coordinate axis, so they have a negative correlation. According to the analysis above, we know that, in lateral (Y_B) component, the movement of the middle span is mainly caused by the wind loads, which accords with other researchers' results (Wang et al., 2016).

According to Meng et al. (2007), the structural mode parameters such as natural frequencies and mode shapes can be extracted from responding measurements under ambient excitation loadings due to their convenience and cost-effectiveness. Figure 11 shows a typical example of extracted natural frequencies and corresponding amplitudes from displacement in lateral (Y_B) direction of

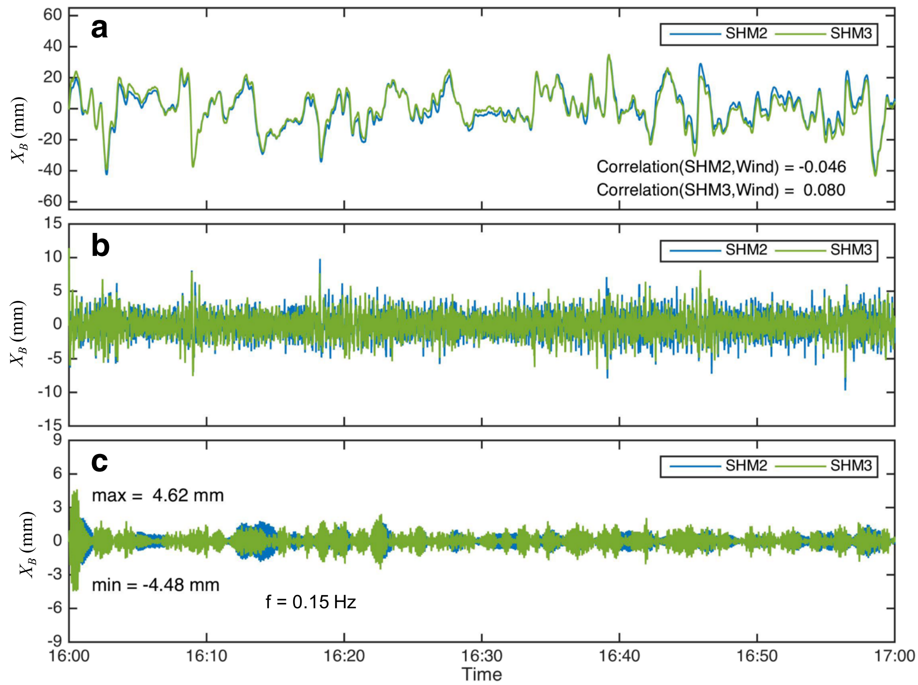

Fig. 14 Long-term (**a**) and vibration signals (**b**) decomposed from longitudinal (X_B) component of middle span, and the dominant frequency signal (**c**) extracted from displacement

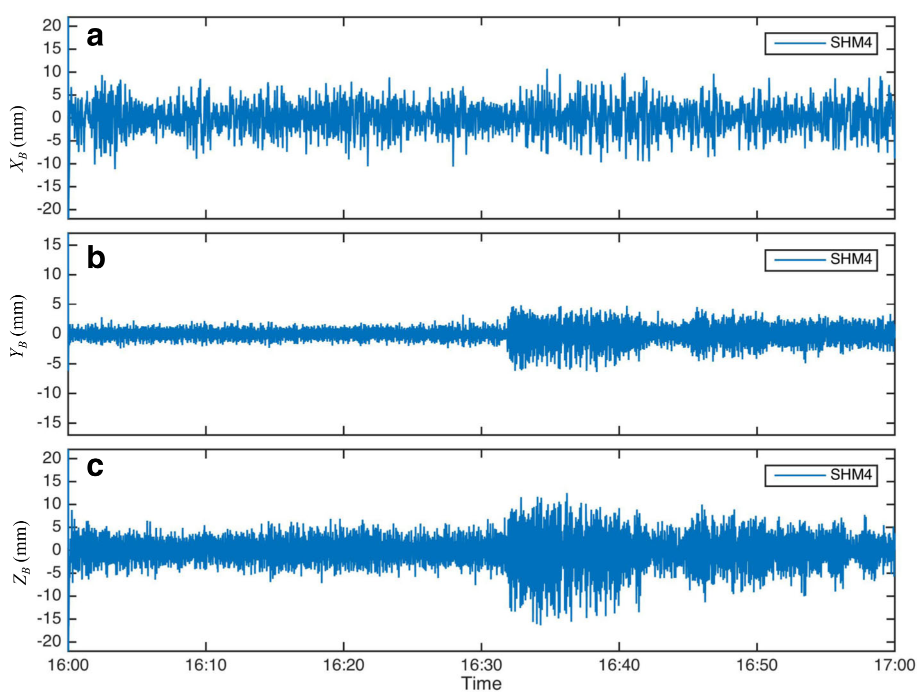

Fig. 15 Dynamic vibration signals for top of the tower

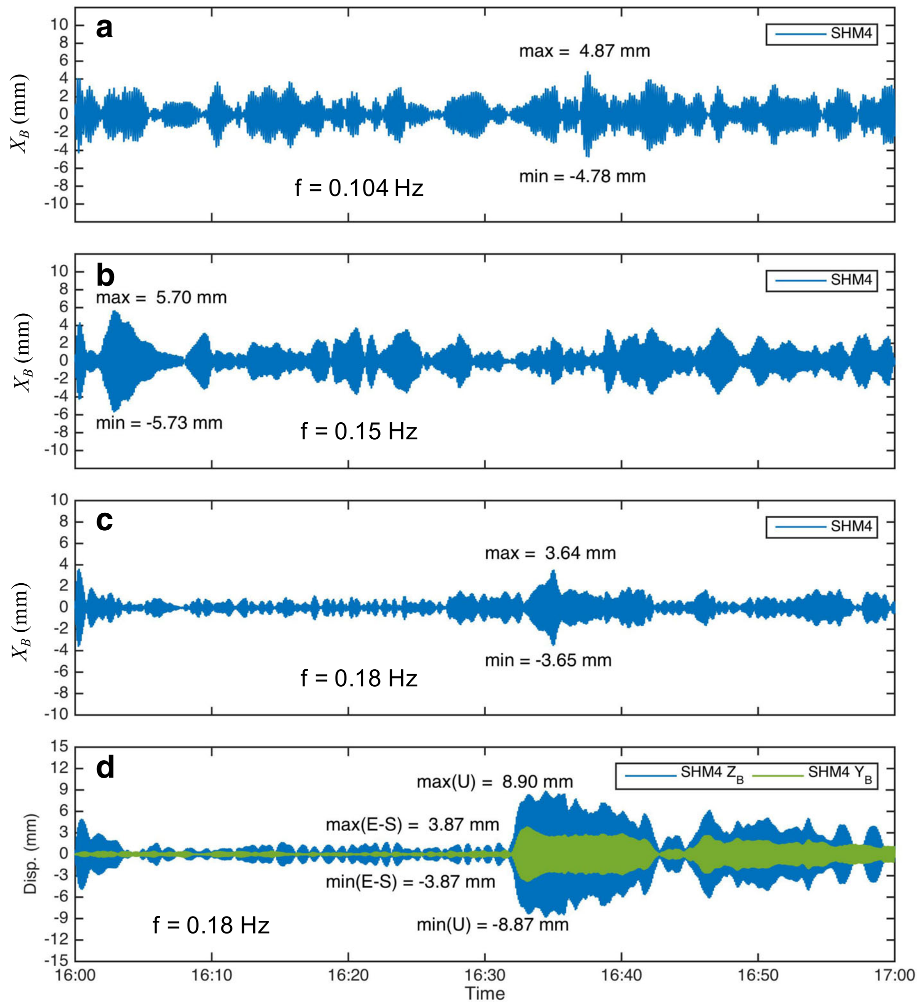

Fig. 16 The dominant frequency signals extracted from displacement of top of the towers. The cutoff elevation is 10° in GPS data processing

the middle span. As Górski (2017) mentioned, the frequency of GNSS time series under 0.05 Hz is mainly trend signal and low frequency background noise. From previous FFT analysis, the dominant frequencies are all over 0.05 Hz and limited to 1.1 Hz. In this case, the time series in lateral (Y_B) direction of the middle span were filtered using the eight-order Type 1 Chebyshev high-pass digital filter with pass-band 0.05 Hz and stop-band 1.1 Hz, which is shown in Fig. 11a-e, show the local frequencies series extracted using a very narrow pass band filter around the dominant frequencies in Table 2. The figure only gives the series when there is the maximum amplitude. As it is shown, the amplitude of first natural frequency under ambient loads is significantly larger than other frequencies. The amplitude of second and third natural frequencies due to wind is at about 1 mm level and the forth is less than 1 mm. That means the first natural frequency is the absolute dominant frequency in the dynamic vibration signal and it should be paid more attention in the SHM.

In the height (Z_B) component of the middle span, traffic loads are the main factors responsible for the displacements (Wang et al., 2016). At the middle span, the displacement in the height direction can reach to 30 cm. Figure 12a gives the long-period component of the displacement time series. The same as lateral (Y_B) direction, the time series for the two stations agree with each other. Because the main cable links the middle span and top of the tower, the displacements in longitudinal (X_B) direction of the tower are shown in Fig. 12b. Based on Eq. (4), the correlation coefficients between the time series of the middle span in Fig. 12a and of the top of the tower were calculated. We can see that the correlation coefficients are − 0.701 and − 0.689, which demonstrates the high correlation between the middle span and the tower.

Figure 13 shows the dynamic vibration response of the middle span in the height (Z_B) component (Fig. 13a) and the time series of dominant frequencies (Fig. 13b-d).

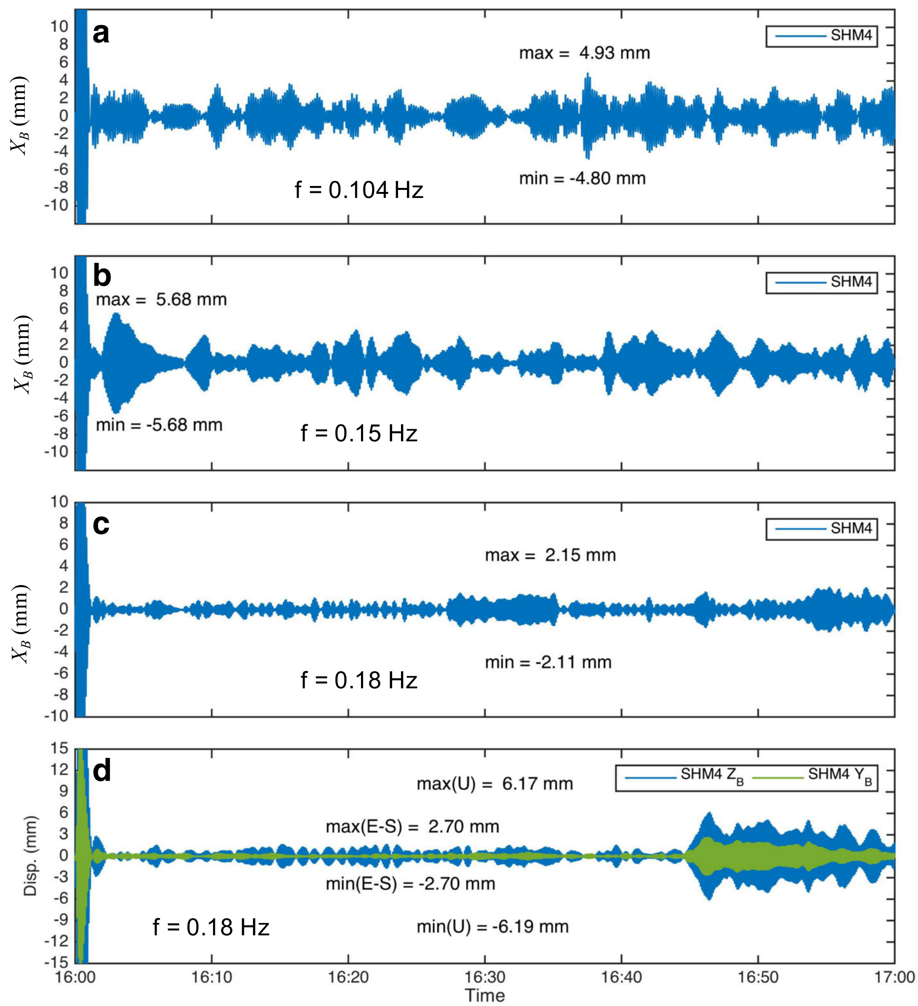

Fig. 17 The dominant frequency signals extracted from displacement of top of the towers. The cutoff elevation is 15° in GPS data processing

From Fig. 13, we know that the first frequency is 0.104 Hz with corresponding maximum amplitude 18 mm under traffic loads. The maximum amplitudes for the other two frequencies 0.205 Hz and 0.268 Hz are about 4 mm. Still, the first natural frequency 0.104 Hz is playing the dominant role in the ambient excitation.

Figure 14 illustrates the longitudinal (X_B) deflections. The changeable range is from 2 cm to 4 cm in the long-period component. The dynamic response is within 5 mm, and the dominant frequency is 0.15 Hz. From the correlation coefficients between the displacement and wind data, the movement of the middle span is almost not dependent on the wind. Due to the stiffness of the bridge, and significantly coupled with that in the height (Z_B) direction, the movement characteristic in the longitudinal (X_B) component is complicated and like a pendulum, which needs more analysis in the future.

As for the tower, the low frequency term in the longitudinal (X_B) has been analysed previously. Due to the stiffness of the tower, for the lateral and height components in Fig. 6, there is no obvious excitation response in the time series. The trend term is mainly because of multipath effect, which can be eliminated by the sidereal filter. The dynamic vibration signals for the three components are shown in Fig. 15. It can be seen that some dynamic responses in the longitudinal (X_B) component can still be noticed. For the lateral (Y_B) and height (Z_B) component, before 16:30, the time series almost demonstrates the white noise characteristics. However, around 16:32, the amplitudes increase significantly.

From Fig. 16d, the amplitude is increasing at the same moment. There are two factors can cause this: the excitations from wind, traffic or other loads and the measurement noise. After checking the wind data in this period, the wind speed and direction did not change and the big excitation from traffic loads is not at this period. Then, we improved the cut-off elevation from 10° to 15° in the GNSS data processing. The same dominant frequencies time series in all three directions are shown in Fig. 17. At the beginning epochs, one or two minutes are needed to fix the ambiguities with the cut-off elevation of 15°. The large amplitude is caused by the float ambiguity resolutions. Except for the beginning time series, we can find that the high amplitude signal between 16:30 and 16:40 is missing in Fig. 17c, d. Then, we checked the satellite number variation during this period. At about 16:31:50, the elevation of G17 was exceeding 10° and began to be used in positioning. As is commonly known, the low elevation signal can easily be contaminated by multipath effect and residual atmospheric delay to contain high-level noise (Amiri-Simkooei and Tiberius, 2007). Therefore, the high-level noise can propagate into the amplitude of vibration frequencies.

Compared Fig. 16a, b with Fig. 17a, b, the excitation moment and amplitude are almost invariant. That means only the natural frequency of the tower was effected by the noise in GNSS measurements. Therefore, more analysis should be done to figure out the effect of noise for dynamic response signal in SHM. However, these issues are beyond the scope of this study.

Conclusions

Structure health monitoring and assessment for large bridges and infrastructures are very important for the life-safety and current or future performance of these systems. The GeoSHM system, conducted by the University of Nottingham, intends to develop and demonstrate a novel system to tackle the issues in structural deformation monitoring of long bridges and make it possible for the bridge masters to fully understand the loading and response effect of the bridge, and identify unusual deformations under extreme weather conditions. Based on the reference monitoring system on the Forth Road Bridge, the paper used the GNSS measurements and corresponding loading data to analyse the dynamic characteristic of the bridge.

To support data analysis, a moving average filter was employed to extract the low frequency of the ambient loading response. The results demonstrate that, the movement of Forth Road Bridge in the lateral (Y_B) component is mainly dependent on the wind, and it has a high correlation with the wind loadings at around 0.7. In the height (Z_B) component, the displacement of middle span under the traffic loadings can reach up to 0.3 m and because of the main cable linking the middle span and top of the tower, the movement time series of the top of the tower in the longitudinal (X_B) direction has a high correlation coefficient with the displacement of the middle span. The displacement can achieve up to 6 cm. In the lateral (Y_B) and height (Z_B) component, due to the stiffness of the tower, the trend term mainly contains multipath effect and possibly the quasi-static displacement.

Then, by FFT algorithm and bandpass filter, the dynamic vibration frequencies and corresponding motion amplitude were extracted from the Forth Road Bridge under ambient excitation loadings. It is found that the first natural frequencies of the middle span of Forth Road Bridge are 0.065 Hz, 0.15 Hz and 0.104 Hz for lateral (Y_B), longitudinal (X_B) and height (Z_B) components respectively. For the south tower, 0.18 Hz can be shown in all three directions, and 0.104 Hz are shown in the longitudinal (X_B) component because of the cables between the tower and middle span. The natural frequency of the longitudinal (X_B) direction of the bridge 0.15 Hz can also be shown in the time series.

From the analysis of this paper, we know that the low frequency response of bridges and dynamic vibration characteristics under ambient loadings can be reflected and extracted by GNSS technology. The monitoring information provided by GNSS is highly meaningful for bridge masters in that they can use these data sources for the decision making of opening or closure and maintenance or repair of the bridge. However, there are still some critical problems to be addressed. For instance, the noisy GNSS measurements increase the amplitudes of vibration frequencies and the second and higher natural frequencies with small dynamic displacements cannot be detected.

In these cases, multi-constellation GNSS systems and integration with other sensors to collect loading and responding data with a high reliability, will be the key for the success of the GeoSHM system. The GeoSHM team includes a variety of experts for geomatics, civil engineering, computer science, communications, etc. With the increase in new large bridges being built in developing countries, especially in China, and some bridges in the developed countries having been in service for more than 50 years, the GeoSHM system becomes more and more important in making sure that large bridges and infrastructures are operating safely.

Acknowledgments

The authors would like to express their gratitude to the European Space Agency for continuously sponsoring the GeoSHM Projects. In addition, Amey PLC., Transport Scotland, China Railway Major Bridge Reconnaissance and Design Institute Co., Ltd. and Panda GNSS Co., Ltd. are acknowledged for their resource inputs. Thank two anonymous reviewers for their very constructive comments.

Funding

This work is supported by "the Open Foundation of Key Laboratory of Precise Engineering and Industry Surveying of National Administration of Surveying, Mapping and Geoinformation" (Grant No. PF2017–8). The Chinese Scholarship Council (CSC) has provided the second author a scholarship which allows him to visit the University of Nottingham for 2 years to research and study in the UK from November 2016.

Authors' contributions

XM proposed the initial idea, built the GeoSHM system and revised this manuscript; RX wrote this paper and analyzed the results of the experiments;

YX carried out the project implementation. All authors read and approved the final manuscript.

Competing interests
The authors declare that they have no competing interests.

Publisher's Note
Springer Nature remains neutral with regard to jurisdictional claims in published maps and institutional affiliations.

Author details
[1]Nottingham Geospatial Institute, The University of Nottingham, Nottingham NG7 2TU, UK. [2]School of Geodesy and Geomatics, Wuhan University, 129 Luoyu Road, Wuhan, Hubei 430079, China.

Received: 21 September 2017 Accepted: 7 March 2018
Published online: 20 March 2018

References

Amiri-Simkooei AR, Tiberius C (2007) Assessing receiver noise using GPS short baseline time series. GPS Solutions 11(1):21–35
Breuer P, Chmielewski T, Górski P et al (2015) Monitoring horizontal displacements in a vertical profile of a tall industrial chimney using global positioning system technology for detecting dynamic characteristics. Struct Control Health Monit 22(7):1002–1023
Elnabwy MT, Kaloop MR, Elbeltagi E (2013) Talkha steel highway bridge monitoring and movement identification using RTK-GPS technique. Measurement 46(10):4282–4292
Erdoğan H, Gülal E (2009) The application of time series analysis to describe the dynamic movements of suspension bridges. Nonlinear Anal Real World Appl 10(2):910–927
Górski P (2017) Dynamic characteristic of tall industrial chimney estimated from GPS measurement and frequency domain decomposition. Eng Struct 148: 277–292
Hristopulos DT, Mertikas SP, Arhontakis I et al (2007) Using GPS for monitoring tall-building response to wind loading: filtering of abrupt changes and low-frequency noise, variography and spectral analysis of displacements. GPS Solutions 11(2):85–95
Li X, Ge L, Ambikairajah E et al (2006) Full-scale structural monitoring using an integrated GPS and accelerometer system. GPS Solutions 10(4):233–247
Meng X (2002) Real-Time Deformation Monitoring of Bridges Using GPS/ Accelerometers. Ph.D. Thesis, University of Nottingham, Nottingham.
Meng X, Dodson AH, Roberts GW (2007) Detecting bridge dynamics with GPS and triaxial accelerometers. Eng Struct 29(11):3178–3184
Meng X, Roberts GW, Dodson AH et al (2004) Impact of GPS satellite and pseudolite geometry on structural deformation monitoring: analytical and empirical studies. J Geod 77(12):809–822
Meng X, Roberts G W, Dodson A H, et al. (2006) GNSS for structural deformation and deflection monitoring: implementation and data analysis. 3rd IAG / 12th FIG Spectrum
Meng X, Wang J, Han H (2014) Optimal GPS/accelerometer integration algorithm for monitoring the vertical structural dynamics. J Appl Geodesy 8(4):265–272
Meng X, Xie Y, Bhatia P, et al (2016) Research and development of a pilot project using GNSS and Earth Observation (GeoSHM) for structural health monitoring of the Forth Road Bridge in Scotland. In Proceedings of the Joint International Symposium on Deformation Monitoring, Vienna, Austria, 30 March–1 April 2016.
Moschas F, Stiros S (2011) Measurement of the dynamic displacements and of the modal frequencies of a short-span pedestrian bridge using GPS and an accelerometer. Eng Struct 33(1):10–17
Moschas F, Stiros S (2014) Dynamic multipath in structural bridge monitoring: an experimental approach. GPS solutions 18(2):209–218
Roberts GW, Brown CJ, Meng X et al (2012) Deflection and frequency monitoring of the forth road bridge, Scotland, by GPS. Proceedings of the Institution of Civil Engineers. Bridg Eng 165(2):105–123
Roberts GW, Cosser E, Meng X, Dodson A (2004) High frequency deflection monitoring of bridges by GPS. J Glob Positioning Syst 3(1–2):226–231
Roberts GW, Meng X, Dodson A (2001) The use of kinematic GPS and triaxial accelerometers to monitor the deflection of large bridges. In Proceedings of the 10th International Symposium on Deformation Measurement, Orange, CA, USA, 19–22 March 2001.
Sumitoro S, Matsui Y, Kono M, et al (2011) Long span bridge health monitoring system in Japan. In: Chase SB, Aktan AE, editors. Health monitoring and management of civil infrastructure systems. Bellingham (WA), The International Society for Optical Engineering. p. 517–24
Tamura Y, Matsui M, Pagnini LC et al (2002) Measurement of wind-induced response of buildings using RTK-GPS. J Wind Eng Ind Aerodyn 90(12): 1783–1793
Wang J, Meng X, Qin C et al (2016) Vibration frequencies extraction of the forth road bridge using high sampling GPS data. Shock Vib 2016:1–18
Watson C, Watson T, Coleman R (2007) Structural monitoring of cable-stayed bridge: analysis of GPS versus modeled deflections. J Surv Eng 133(1):23–28
Xiong C, Lu H, Zhu J (2017) Operational modal analysis of bridge structures with data from GNSS/accelerometer measurements. Sensors 17(3):436
Xu L, Guo JJ, Jiang JJ (2002) Time–frequency analysis of a suspension bridge based on GPS. J Sound Vib 254(1):105–116
Yi TH, Li HN, Gu M (2013) Experimental assessment of high-rate GPS receivers for deformation monitoring of bridge. Measurement 46(1):420–432
Yu J, Meng X, Shao X et al (2014) Identification of dynamic displacements and modal frequencies of a medium-span suspension bridge using multimode GNSS processing. Eng Struct 81:432–443
Yu J, Yan B, Meng X et al (2016) Measurement of bridge dynamic responses using network-based real-time kinematic GNSS technique. J Surv Eng 142(3): 04015013